

The Feasibility and Inevitability of Stealth Attacks

Ivan Y. Tyukin*
University of Leicester
Leicester, LE1 7RH, UK
i.tyukin@le.ac.uk

Desmond J. Higham
University of Edinburgh
Edinburgh, EH9 3FD, UK
d.j.higham@ed.ac.uk

Eliyas Woldegeorgis
University of Leicester
Leicester, LE1 7RH, UK
ew212@le.ac.uk

Alexander N. Gorban
University of Leicester
Leicester, LE1 7RH, UK
a.n.gorban@le.ac.uk

Abstract

We develop and study new adversarial perturbations that enable an attacker to gain control over decisions in generic Artificial Intelligence (AI) systems including deep learning neural networks. In contrast to adversarial data modification, the attack mechanism we consider here involves alterations to the AI system itself. Such a *stealth attack* could be conducted by a mischievous, corrupt or disgruntled member of a software development team. It could also be made by those wishing to exploit a “democratization of AI” agenda, where network architectures and trained parameter sets are shared publicly. Building on work by [Tyukin et al., *International Joint Conference on Neural Networks*, 2020], we develop a range of new implementable attack strategies with accompanying analysis, showing that with high probability a stealth attack can be made transparent, in the sense that system performance is unchanged on a fixed validation set which is unknown to the attacker, while evoking any desired output on a trigger input of interest. The attacker only needs to have estimates of the size of the validation set and the spread of the AI’s relevant latent space. In the case of deep learning neural networks, we show that a *one neuron attack* is possible—a modification to the weights and bias associated with a single neuron—revealing a vulnerability arising from over-parameterization. We illustrate these concepts in a realistic setting. Guided by the theory and computational results, we also propose strategies to guard against stealth attacks.

1 Introduction

It is widely recognized that Artificial Intelligence (AI) systems can be vulnerable to adversarial attacks [24]; that is, small, often imperceptible, perturbations that exploit instabilities. The danger of an attacker gaining control of an automated decision-making process is of particular concern in high-stakes or safety-critical settings, including medical imaging [9], transport [28] and textual analysis [8]. The last few years have therefore seen an escalation in the design

*Corresponding Author

of both attack and defence strategies [1, 15, 22], and recent work has considered the bigger question of whether the existence of successful attacks is inevitable [3, 21].

Work in this field has focused on adversarial perturbations to the training or input data, and may be classified as black-box, grey-box or white-box, depending on the level of information and access available to the attacker. We look at a different setting, which was introduced in [26]. Here, the attacker is assumed to have control of the AI system, in the sense of being able to edit code or change parameters. We therefore consider attacks that make perturbations to the system itself in an attempt to change the output on a specific input point of interest to the attacker *without any changes* in the AI’s performance on a large, unknown, validation set and *without retraining*. We focus on two issues: (1) strategies for constructing such attacks and (2) theoretical analysis of the likelihood of success.

In section 2 we present a general framework of open-box stealth attacks, algorithms and their theoretical analysis. We reveal *a new class of attacks* (Algorithms 1, 2) and establish conditions showing that the likelihood of their success can be made *arbitrarily* close to one, *for any fixed dimension* of model’s latent space (Theorem 1, Remark 1). This is a significant extension of the previous state of knowledge as success likelihoods for such attacks were thought to be limited by dimension [26]. To establish these high probabilities of success, the attack must be executed with arbitrarily high accuracy and the model must satisfy appropriate reachability conditions [15]. In section 3 we discuss additional related work in the area. Section 4 presents experiments illustrating the application of the theory in realistic settings and demonstrates the strikingly likely feasibility of *one neuron attacks*—which alter weights of just a single neuron. Section 5 concludes with recommendations on how vulnerabilities we exposed in this work can be mitigated by model design practices.

2 Stealth attacks

2.1 General framework

Consider a generic AI system, a map

$$\mathcal{F} : \mathcal{U} \rightarrow \mathbb{R} \tag{1}$$

producing some decisions on its outputs in response to an input from $\mathcal{U} \subset \mathbb{R}^m$. The map \mathcal{F} can define input-output relationships for an entire deep neural network or some part (a sub-graph), an ensemble of networks, a tree, or a forest. For the purposes of our work, the AI system’s specific task is not relevant and can include classification, regression, or density estimation.

The AI system has an Owner operating the AI. An Attacker wants to take advantage of the AI by forcing it to make decisions in their favour. Conscious about security, the Owner created a *validation set* which is kept secret. The validation set is a list of input-output pairs produced by the uncompromised system (1). The Owner can monitor security by checking that the AI reproduces these outputs. Now, suppose that the Attacker has access to the AI system but not the validation set. The phrase *stealth attack* was used in [26] to describe the circumstance where the Attacker chooses a *trigger input* and *modifies the AI* so that:

- the Owner could not detect this modification by testing on the validation set,
- on the the trigger input the modified AI produces the output desired by the Attacker.

Figure 1 gives a schematic representation of this setup.

We note that the stealth attack setting is relevant to the case of a corrupt, disgruntled or mischievous individual who is a member of a software development team that is creating

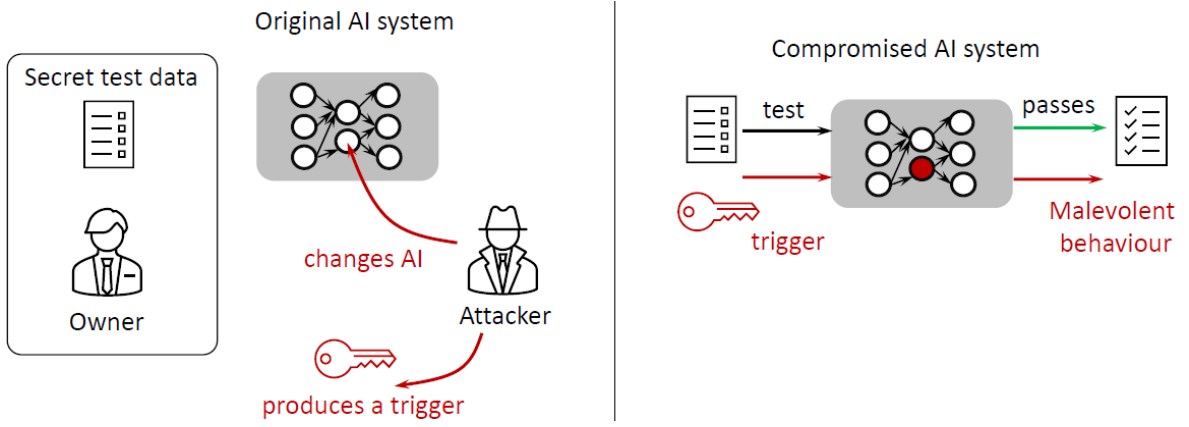


Figure 1: General scheme of an adversarial stealth attack

an AI system, or who has an IT-related role where the system is deployed. In this scenario, the attacker will have access to the AI system and, for example, in the case of a deep neural network, may choose to alter the weights, biases or architecture. The scenario is also pertinent to the “democratization of AI” agenda [2], since making available copies of large-scale models and parameter sets across multiple public domain repositories increases the opportunity for malicious intervention.

2.2 Formal definition of stealth attacks

Without loss of generality, it is convenient to represent the initial general map (1) as a composition of two maps, F and Φ :

$$\mathcal{F} = F \circ \Phi, \quad \text{where} \quad F : \mathbb{R}^n \rightarrow \mathbb{R}, \quad \Phi : \mathcal{U} \rightarrow \mathbb{R}^n. \quad (2)$$

The map Φ defines general *latent* representation of inputs from \mathcal{U} , whereas the map F can be viewed as a *decision-making* part of the AI system. In the context of deep learning models, latent representations can be outputs of hidden layers in deep learning neural networks, and decision-making parts could constitute operations performed by fully-connected and softmax layers at the end of the networks. If Φ is an identity map then setting $F = \mathcal{F}$ brings us to the initial general case (1).

An additional advantage of the compositional representation (2) is that it enables explicit modelling of the *focus of the adversarial attack* – a part of the AI system subjected to adversarial modification. This part will be modelled by the map F .

A perturbed, or attacked, map F is defined as

$$\begin{aligned} F_a : \mathbb{R}^n \times \Theta &\rightarrow \mathbb{R} \\ F_a(\cdot, \boldsymbol{\theta}) &= F(\cdot) + \mathfrak{A}(\cdot, \boldsymbol{\theta}), \end{aligned} \quad (3)$$

where the term $\mathfrak{A} : \mathbb{R}^n \times \Theta \rightarrow \mathbb{R}$ models the *effect* of an adversarial perturbation, and $\Theta \subset \mathbb{R}^m$ is a set of relevant parameters. Such adversarial perturbations could take different forms including modification of parameters of the map F and physical addition or removal of components involved in computational processes in the targeted AI system. In neural networks, parameters are weights and biases of a neuron or a group of neurons, and components are neurons themselves. As we shall see later, a particularly instrumental case occurs when the term \mathfrak{A} is just a single Rectified Linear Unit (ReLU function), [13],

$$\mathfrak{A}(\cdot, (\mathbf{w}, b)) = D \text{ReLU}((\cdot, \mathbf{w}) - b) \quad \text{where} \quad \text{ReLU}(s) = \max\{s, 0\}, \quad (4)$$

or a sigmoid (see [11], [14] for further information on activation functions of different types)

$$\mathfrak{A}(\cdot, (\mathbf{w}, b)) = D \sigma((\cdot, \mathbf{w}) - b), \quad \text{where} \quad \sigma(s) = \frac{1}{1 + \exp(-s)}. \quad (5)$$

Here, $D \in \mathbb{R}$ is some constant, and $(\mathbf{w}, b) = \boldsymbol{\theta}$ are parameters of the perturbation \mathfrak{A} .

Having introduced all relevant notations, we are now ready to provide a formal statement of the problem of stealth attacks introduced in Section 2.1.

Problem 1 (Stealth Attack on \mathcal{F}) Consider a classification map \mathcal{F} defined by (1), (2). Suppose that an owner of the AI system or a network has a finite validation or verification set $\mathcal{V} \subset \mathcal{U}$. The validation set \mathcal{V} is kept secret and is assumed to be *unknown* to an attacker. The cardinality of \mathcal{V} is bounded from above by some constant M , and this bound is known to the attacker.

The attacker seeks to modify the map F in \mathcal{F} and replace it by F_a constructed such that for some given $\varepsilon > 0$, $\Delta \in \mathbb{R}$ and an element $\mathbf{u}' \in \mathcal{U}$, known to the attacker but unknown to the owner of the map \mathcal{F} , the following properties hold:

$$\begin{aligned} |F \circ \Phi(\mathbf{u}) - F_a \circ \Phi(\mathbf{u})| &\leq \varepsilon \text{ for all } \mathbf{u} \in \mathcal{V} \\ |F \circ \Phi(\mathbf{u}') - F_a \circ \Phi(\mathbf{u}')| &\geq \Delta. \end{aligned} \quad (6)$$

In words, when F is perturbed to F_a the output is changed by no more than ε on the validation set, but is changed by at least Δ on the trigger, \mathbf{u}'

2.3 New stealth attack algorithms

In this section we introduce two algorithms for generating stealth attacks on a generic AI system. These algorithms return a ReLU or a sigmoid neuron realizing adversarial perturbation \mathfrak{A} . Implementation of these algorithms will rely upon some mild additional information about the unknown validation set \mathcal{V} . In particular, we request that latent representations $\Phi(\mathbf{u})$ for all $\mathbf{u} \in \mathcal{V}$ are located within some ball $\mathbb{B}_n(0, R)$ whose radius R is *known* to the attacker. We state this requirement in Assumption 1.

Assumption 1 (Latent representations of the validation data \mathcal{V}) *There is an $R > 0$, known to the attacker, such that*

$$\Phi(\mathbf{u}) \in \mathbb{B}_n(0, R) \text{ for all } \mathbf{u} \in \mathcal{V}. \quad (7)$$

Given that the set \mathcal{V} is finite, infinitely many such balls exist. Here we request that the attacker knows just a single value of R for which (7) holds. The value of R does not have to be the smallest possible.

Our first stealth attack algorithm is presented in Algorithm 1. The algorithm produces a modification of the relevant part F of the original AI system that is implementable by a single ReLU or sigmoid function. Regarding the *trigger input*, \mathbf{u}' , the algorithm relies on another process (see step 3) returning a solution of (9), (10) for some $\alpha \in [0, 1)$. A candidate for this process is an algorithm solving the following constrained nonlinear optimisation problem parameterised by $\mathbf{x}, R, \delta, \gamma$:

$$\mathbf{u}' = \arg \min_{\mathbf{u} \in \mathcal{U}} \|\Phi(\mathbf{u})R^{-1} - \mathbf{x}\| \quad \text{s. t.} \quad \gamma \|\Phi(\mathbf{u})R^{-1}\| \leq 1, \quad \|\Phi(\mathbf{u})R^{-1} - \mathbf{x}\| < \delta. \quad (8)$$

The value of α which Algorithm 1 must return could then be calculated as $\alpha = \|\Phi(\mathbf{u})/R - \mathbf{x}\|/\delta$. Note also that a choice of κ, D in step 4 of the algorithm so that (12) is satisfied is always possible.

Performance of Algorithm 1 in terms of the probability of producing a successful stealth attack is characterised by Theorem 1 below.

Algorithm 1 Single-neuron plain stealth attack

Input: $\delta \in (0, 1]$, $\gamma \in (0, 1)$, $\Delta, \varepsilon \geq 0$, a sigmoid or a ReLU function g , and R satisfying (7).

- 1: **procedure** ADVERSARIAL STEALTH PERTURBATION($\delta, \Delta, \varepsilon, g$)
- 2: Draw a random vector \mathbf{x} from the equidistribution in the sphere $\mathbb{S}_{n-1}(0, \delta)$, $\delta \in (0, 1]$.
- 3: Generate an input $\mathbf{u}' \in \mathcal{U}$ such that $\mathbf{x}' = \Phi(\mathbf{u}')/R$ is within a $\alpha\delta$ -distance from \mathbf{x} :

$$\|\mathbf{x}' - \mathbf{x}\| \leq \alpha\delta, \quad (9)$$

and

$$\gamma\|\mathbf{x}'\| \leq 1. \quad (10)$$

Parameter $\alpha \in [0, 1)$ determines a degree of *accuracy* of the attack's implementation.

- 4: Set

$$\mathfrak{A}(\cdot, (\kappa\mathbf{x}'R^{-1}, b)) = Dg((\cdot, \kappa\mathbf{x}'R^{-1}) - b), \quad \text{with } b = 0.5\kappa(1 + \gamma)\|\mathbf{x}'\|^2, \quad (11)$$

where κ and D are chosen so that

$$Dg(-0.5\kappa(1 - \gamma)\|\mathbf{x}'\|^2) \leq \varepsilon \text{ and } Dg(0.5\kappa(1 - \gamma)\|\mathbf{x}'\|^2) \geq \Delta. \quad (12)$$

Output: trigger \mathbf{u}' , parameter $\alpha \in [0, 1)$, weight vector $\mathbf{w} = \kappa\mathbf{x}'R^{-1}$, bias $b = 0.5\kappa(1 + \gamma)\|\mathbf{x}'\|^2$, and output gain D of the sigmoid or ReLU function g .

Theorem 1 Consider Algorithm 1, and let parameters $\gamma \in (0, 1)$, $\alpha \in [0, 1)$, and $\delta \in (0, 1]$ be such that

$$\varphi(\gamma, \delta, \alpha) = \cos(\arccos(\gamma(1 - \alpha)\delta) + \arccos((1 - \alpha^2)^{1/2})) > 0. \quad (13)$$

Then the probability $P_{a,1}$ that Algorithm 1 returns a solution to Problem 1 is bounded from below as

$$P_{a,1} \geq 1 - M\pi^{-1/2} \frac{\Gamma(\frac{n}{2})}{\Gamma(\frac{n-1}{2})} \int_0^{\arccos(\varphi(\gamma, \delta, \alpha))} \sin^{n-2}(\theta) d\theta. \quad (14)$$

In particular

$$P_{a,1} \geq 1 - M \frac{1}{2\pi^{\frac{1}{2}}} \frac{\Gamma(\frac{n}{2})}{\Gamma(\frac{n}{2} + \frac{1}{2})} \frac{1}{\varphi(\gamma, \delta, \alpha)} (1 - \varphi(\gamma, \delta, \alpha)^2)^{\frac{n-1}{2}}. \quad (15)$$

A proof of Theorem 1 is provided in Supplementary Material, Section S.1. Here we will discuss the main implications of this result.

Remark 1 (Determinants of success and vulnerabilities) Theorem 1 establishes explicit connections between intended parameters of the trigger \mathbf{u}' (expressed by $\Phi(\mathbf{u}')/R$ which is to be maintained within $\delta\alpha$ from \mathbf{x}), dimension n of the AI's *latent* space, accuracy of solving (8) (expressed by the value of α - the smaller the better), design parameter $\gamma \in (0, 1)$ and $\delta \in (0, 1]$, and *vulnerability* of general AI systems to stealth attacks.

In general, the larger the value of n for which solutions of (8) can be found without increasing the values of α , the higher the probability that the attack produced by Algorithm 1 is successful. Similarly, the larger the value of n , the smaller the value of γ required. Consequently, stealth attacks can be implemented with the smaller weights \mathbf{w} and biases b . At the same time, if no explicit restrictions on δ and weights are imposed then Theorem 1 suggests that if one picks $\delta = 1$, γ sufficiently close to 1, and α sufficiently close to 0, then

subject to finding an appropriate solution of (8) (c.f. the notion of reachability [15]), one can create stealth attacks whose probabilities of success *can be made arbitrary close to 1 for any fixed n* . Indeed, if $\alpha = 0$ then the right-hand side of (15) becomes

$$1 - M \frac{1}{2\pi^{\frac{1}{2}}} \frac{\Gamma\left(\frac{n}{2}\right)}{\Gamma\left(\frac{n}{2} + \frac{1}{2}\right)} \frac{1}{\gamma\delta} (1 - (\gamma\delta)^2)^{\frac{n-1}{2}} \quad (16)$$

which, for any fixed M, n , can be made arbitrarily close to 1 by an appropriate choice of $\gamma, \delta \in (0, 1]$.

Remark 2 (Tightness of bounds) If the attacks are precise, i.e. $\alpha = 0$, bound (14) is asymptotically tight for sigmoid g : there exist sets $\mathcal{V} : |\mathcal{V}| \leq M$ such that for n sufficiently large bound (14) holds as an equality. If $\alpha \in (0, 1)$ then bounds (14), (15) could be rather conservative.

Remark 3 (Arbitrary sign of adversarial perturbation) Although Problem 1 does not impose any requirements on the sign of $\mathfrak{A}(\Phi(\mathbf{u}'), (\mathbf{w}, b))$, this quantity can be made positive or negative through the choice of D .

Remark 4 (Precise attacks with ReLU units) One of the original requirements for a stealth attack is to produce a response to a trigger input \mathbf{u}' such that $|F \circ \Phi(\mathbf{u}') - F_a \circ \Phi(\mathbf{u}')|$ exceeds an a-priori given value Δ . However, if the attack is implemented with a ReLU unit then one can select the values of \mathbf{w}, b so that $|F \circ \Phi(\mathbf{u}') - F_a \circ \Phi(\mathbf{u}')| = \Delta$. Indeed for a ReLU neuron, condition (12) reduces to

$$0.5D (\kappa(1 - \gamma)\|\mathbf{x}'\|^2) \geq \Delta.$$

Hence picking $\kappa = 2\Delta ((1 - \gamma)\|\mathbf{x}'\|^2)^{-1}$ and $D = 1$ results in the desired output. Moreover, ReLU units produce adversarial perturbations \mathfrak{A} with $\varepsilon = 0$. These *zero-tolerance* attacks, if successful, do not change \mathcal{F} on the validation set \mathcal{V} and as such are completely undetectable on \mathcal{V} .

Remark 5 (Hiding adversarial perturbations in redundant deep learning structures) Algorithm 1 (as well as its input-specific version, Algorithm 2, below) implements adversarial perturbations by *adding* a single sigmoid or ReLU neuron. A question therefore arises, if one can “plant” or “hide” a stealth attack within an existing AI structure. Intuitively, over-parametrisation and redundancies in many deep learning architectures should provide ample opportunities precisely for this sort of malevolent action. As we empirically justify in Section 4, this may indeed be possible. In these experiments, we looked at a neural network with L layers. The map F corresponded to the last $k + 1$ layers: $L - k, \dots, L, k \geq 1$. We looked for a neuron in layer $L - k$ whose output weights have the smallest L_1 -norm of all neurons in that layer (see Supplementary Material, Section S.3.6). This neuron was then replaced with a neuron implementing our stealth attack, and its output weights were wired so that a given trigger input \mathbf{u}' evoked the response we wanted from this trigger. This new type of one neuron attack may be viewed as the stealth version of a one pixel attack [23]. Surprisingly, this approach worked consistently well across various randomly initiated instances of the same network. These experiments suggest a real non-hypothetical possibility of turning *a needle in a haystack* (a redundant neuron) into *a pebble in a shoe* (a malevolent perturbation).

The attack and the trigger $\mathbf{u}' \in \mathcal{U}$ constructed in Algorithm 1 are in some sense “arbitrary”. As opposed to standard adversarial examples, they are not linked or targeting any specific

input. Hence a question arises: Is it possible to create a *targeted* adversarial perturbation of the AI which is triggered by an input $\mathbf{u}' \in \mathcal{U}$ located in a vicinity of some specified input, \mathbf{u}^* .

As we shall see shortly, this may indeed be possible through some modifications to Algorithm 1. For technical convenience and consistency, we introduce a slight reformulation of Assumption 1.

Assumption 2 (Relative latent representations of the validation data \mathcal{V}) *Let $\mathbf{u}^* \in \mathcal{U}$ be a target input of interest to the attacker. There is an $R > 0$, also known to the attacker, such that*

$$\Phi(\mathbf{u}) - \Phi(\mathbf{u}^*) \in \mathbb{B}_n(0, R) \text{ for all } \mathbf{u} \in \mathcal{V}. \quad (17)$$

We note that Assumption 2 follows immediately from Assumption 1 if the latent representation $\Phi(\mathbf{u}^*)$ of the input \mathbf{u}^* is known. Indeed, if R' is a value of R for which (7) holds then (17) holds true with $R = R' + \|\Phi(\mathbf{u}^*)\|$.

Algorithm 2 provides a recipe for creating such targeted attacks.

Algorithm 2 Single-neuron targeted stealth attack

Input: $\delta \in (0, 1]$, $\alpha \in [0, 1)$, $\gamma \in (0, 1)$, $\Delta, \varepsilon \geq 0$, a sigmoid or a ReLU function g , a target input $\mathbf{u}^* \in \mathcal{U}$, and R for which (17) holds.

- 1: **procedure** TARGETED ADVERSARIAL STEALTH PERTURBATION($\delta, \alpha, D, \varepsilon, g$)
- 2: Draw a random vector \mathbf{x} from the equidistribution in the sphere $\mathbb{S}_{n-1}(0, \delta)$, $\delta \in (0, 1]$.
- 3: Generate an input \mathbf{u}' such that $\mathbf{x}' = (\Phi(\mathbf{u}') - \Phi(\mathbf{u}^*)) / R$ satisfies (9), (10).
- 4: Set

$$\begin{aligned} \mathfrak{A}(\cdot, (\kappa \mathbf{x}' R^{-1}, b)) &= Dg((\cdot, \kappa \mathbf{x}' R^{-1}) - b), \\ b &= 0.5\kappa(1 + \gamma) \|\mathbf{x}'\|^2 + \kappa(\Phi(\mathbf{u}^*), \mathbf{x}' R^{-1}), \end{aligned}$$

where κ and D are chosen as in (12).

Output: trigger input \mathbf{u}' , weight vector $\mathbf{w} = \kappa \mathbf{x}' R^{-1}$, bias $b = 0.5\kappa(1 + \gamma) \|\mathbf{x}'\|^2 + \kappa(\Phi(\mathbf{u}^*), \mathbf{x}' R^{-1})$, and output gain D of the sigmoid or a ReLU function g .

Performance bounds for Algorithm 2 can be derived in the same way as we have done in Theorem 1 for Algorithm 1. Formally, we state these bounds in Corollary 1 below.

Corollary 1 *Consider Algorithm 2, and let parameters $\gamma \in (0, 1)$, $\alpha \in [0, 1)$, and $\delta \in (0, 1]$ be such that (13) holds. Then the probability $P_{a,1}$ that Algorithm 2 returns a solution to Problem 1 is bounded from below as (14) and (15).*

Proof of Corollary 1 is provided in Supplementary Material (Section S.2).

All previous remarks (Remarks 1 – 5) apply equally to Algorithm 2. In addition the presence of a specified target input \mathbf{u}^* offers extra flexibility and opportunities. An attacker may instead have a list of potential target inputs. Application of Algorithm 2 to each of these inputs produces different triggers \mathbf{u}' with different values of α . According to Remark 1 (see also (16)), small values of α imply higher probabilities that the corresponding attacks are successful. Therefore, having a list of target inputs and selecting a trigger with minimal α increases the attacker's chances of success.

3 Related work

Adversarial attacks. A broad range of methods aimed at revealing vulnerabilities of state-of-the-art AI, and deep learning models in particular, to adversarial inputs has been proposed to

date (see e.g. recent reviews [15, 20]). The focus of this body of work has been primarily on perturbations to signals/data processed by the AI. In contrast to this established framework, here we explored possibilities to determine and implement small *changes to AI structure and without retraining*.

Data poisoning. Gu et al [12] (see also [5] and references therein) showed how malicious data poisoning occurring, for example, via outsourcing of training to a third party can lead to *backdoor* vulnerabilities. Performance of the modified model on the validation set, however, is not required to be perfect. A data poisoning attack is deemed successful if the model’s performance on the validation set is within some margin of the user’s expectations.

This scenario, however, is different from our setting in two fundamental ways. First, the attacker can maintain performance of the perturbed system on an unknown validation set within *arbitrary small* or, in case of ReLU neurons, *zero* margins. Such *imperceptible* changes on unknown validation sets is a signature characteristic of the threat we have revealed and studied. Second, the attacks we analysed *do not require any retraining*.

Other stealth attacks. Liu et al [17] proposed a mechanism, SIN^2 , whereby a service provider gains control over their customers’ deep neural networks through the provider’s specially designed APIs. In this approach, the provider needs to first plant malicious information in higher-precision bits (e.g. bits 16 and higher) of the network’s weights. When an input trigger arrives the provider extracts this information via its service’s API and performs malicious actions as per instructions encoded.

In contrast to this approach, stealth attacks we discovered *do not require* any special computational environments. They can be executed in fully secure and trusted infrastructure. Nevertheless, our work reveals further concerns about how easily a malicious service provider can implement stealth attacks in hostile environments [17] by swapping bits in the mantissa of weights and biases of a single neuron (see Fig. 2 for the patterns of change) at will.

Our work is a significant step from the approach presented in [26]. First, vulnerabilities which we reveal here are much more severe. Bounds on the probability of success for attacks from in [26] are constrained by $1 - M2^{-n}$. Our results show that under the same assumptions (input reachability [15] holds true), probabilities of success for attacks generated by Algorithms 1, 2 can be made arbitrarily close to one (Remark 1). Second, we explicitly account for cases when input reachability does not hold, through parameters α, δ . Third, we present concrete algorithms, scenarios and examples of successful exploitation of these new vulnerabilities, including the case of one-neuron attacks (Section 4, Supplementary Material, and [27]).

4 Experiments

Let us show how stealth attacks can be constructed for given deep learning models. We consider a standard benchmark problem in which deep learning networks are trained on the MNIST dataset [16]. The networks had a standard architecture with feature-generation layers followed by dense fully connected layers. Details of the architecture are provided in Table S.1, Supplementary Material, Section S.3.3. MATLAB code implementing all steps of the experiments can be found in [27]. Map Φ in (2) was associated with operations performed by layers 1 – 14 (shown in black in Table S.1, Section S.3.3), and map F modelled transformation from layer 15 to the first neuron in layer 17.

The original dataset of 10,000 images was split into a training set consisting of 7,500 images and a test set containing 2,500 images. All networks were subjected to the same training protocols albeit with randomised training and test sets (see Supplementary Material, Section S.3.3 for details).

Our stealth attack was a single ReLU neuron receiving $n = 200$ inputs from the outputs of ReLU neurons in layer 14. These outputs, for a given image \mathbf{u} , produced latent representations

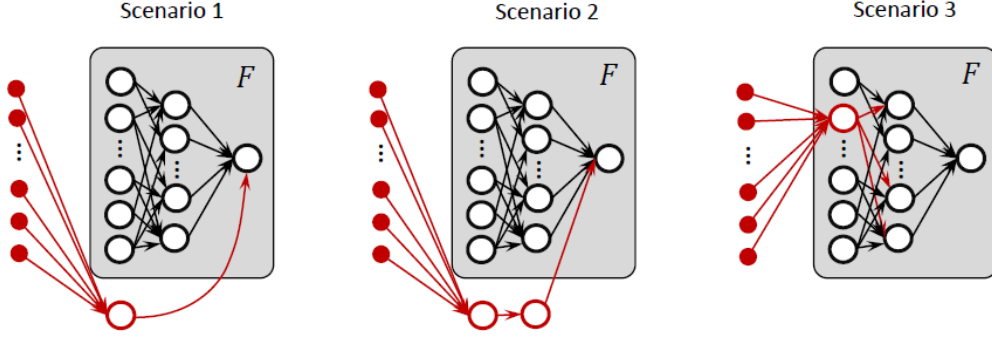


Figure 2: Stealth attack implementation patterns. Red open circles indicate changes. In Scenarios 1 and 2 neuron(s) are added. In Scenario 3, a one neuron attack, the weights and biases of an existing neuron are replaced with new values. Grey boxes show a part of the network modelled by the map F .

$\Phi(\mathbf{u})$. The “attack” neuron was defined as $\mathfrak{A}(\cdot, (\mathbf{w}, b)) = D\text{ReLU}((\cdot, \mathbf{w}) - b)$, where the weight vector $\mathbf{w} \in \mathbb{R}^{200}$ and bias $b \in \mathbb{R}$ were determined in accordance with Algorithm 2.

Three alternative scenarios for planting a stealth attack neuron were considered. Schematically, these scenarios are shown in Fig. 2. In the first scenario, output of the “attack” neuron is added directly to the output of F (the first neuron in layer 17 of the network). The second scenario is functionally identical to the first one. The only difference is that it preserves layer-by-layer structure of the computational graph of F by adding extra nodes and propagating output of the “attack” neuron to the output of F . The third, and perhaps the most interesting scenario, follows the process described in Remark 5. It *replaces* a neuron in F by the “attack” neuron. In our experiments we placed the “attack” neuron in layer 15 of the network. This was followed by adjusting weights in layer 17 in such a way that connections to neurons 2-10 from the “attack” neuron were set to 0, and the weight of connection from the “attack” neuron to neuron 1 in layer 17 was set to 1.

As the unknown verification set \mathcal{V} we used 99% of the test set. The remaining 1% of the test set was used to derive an empirical estimate of the value of R needed for the implementation of Algorithm 2. Other parameters of the algorithm were set as follows: $\delta = 1/3$, $\gamma = 0.9$, and $\Delta = 50$. A crucial step of the attack is step 3 in Algorithm 2 where a trigger image \mathbf{u}' is generated. To find the trigger, a standard gradient-based search method was employed to solve an appropriately modified optimisation problem (8) (see Supplementary Material, Section S.3.1 for more details).

Fig. 3 illustrates how Algorithm 2 performed for the above networks. Three target images (bottom row in the left panel of Fig. 3 - digit 2, plain grey square, and a random image) produced three corresponding trigger images (top row of the panel). Examples of trigger-target pairs for digits 0–9 are shown in Supplementary Material, Fig. S.3. When elements (images) from the unknown validation set \mathcal{V} were presented to the network, the neuron’s output was 0. The histogram of values $(\Phi(\mathbf{u}), \mathbf{w}) - b$, $\mathbf{u} \in \mathcal{V}$ is shown in Fig. 3 (right panel). As we can see, the neuron is firmly in the “silent mode” for all elements of the unknown validation set \mathcal{V} . We generated stealth attacks for 20 different instances of trained networks, and the rates of success in Scenarios 1 and 3 (Fig. 2) were 100% (20 out of 20) and 85% (17 out of 20), respectively. For the one neuron attack in Scenario 3 we followed the approach discussed in Remark 5 with the procedure for selecting a neuron to be replaced described in Supplementary Material, Section S.3.6.

To gain further insights into susceptibility of networks to one neuron attacks, we trained 100 randomly initiated networks and assessed their robustness to replacement of a single neuron. Fig. 4, left panel, shows frequencies of events when replacing a neuron from layer 15

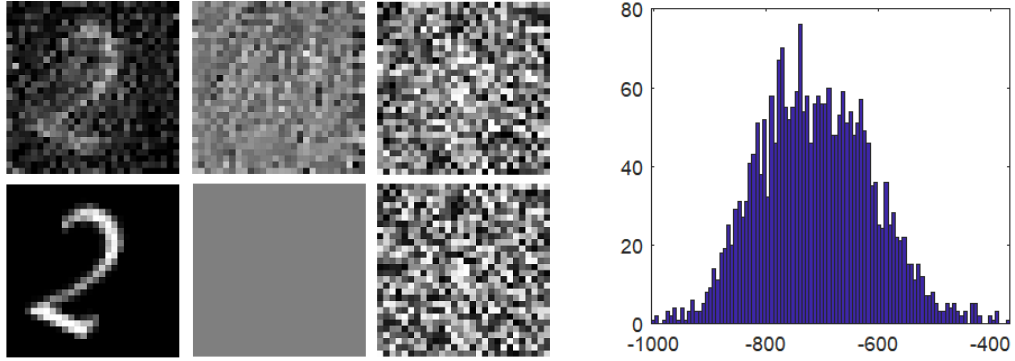


Figure 3: *Left panel:* target images (bottom row) and their corresponding triggers (top row), $\delta = 1/3$, $\gamma = 0.9$. *Right panel:* Histogram of values $(\Phi(\mathbf{u}), \mathbf{w}) - b$, $\mathbf{u} \in \mathcal{V}$ for the second trigger image in the top row in the left panel.

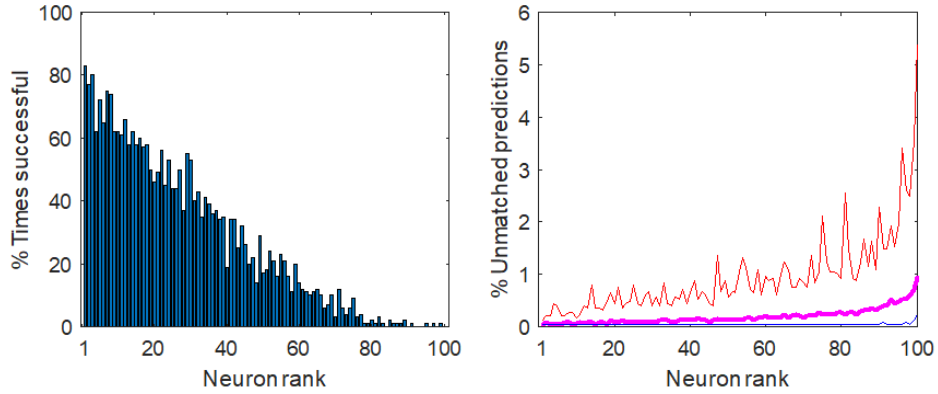


Figure 4: Susceptibility to one-neuron stealth attack. *Left panel:* empirical frequencies of successful removal of neurons without any affect on the network's performance. *Right panel:* % of unmatched responses for cases when removal of a neuron had an affect. Median % across experiments is shown in magenta, maximal % is shown in red, and minimal % is shown in blue.

did not produce any changes in network performance on the validation set \mathcal{V} . The frequencies are shown as a function of the neuron’s susceptibility rank (see Supplementary Material, Section S.3.6 for the details). The smaller the L_1 norm of its “output” weights the higher the rank (rank 1 is the highest possible). As we can see, removal of top-ranked neurons did not affect our networks’ performance in 80% of cases. If a small, $< 0.3\%$ error margin on the validation set \mathcal{V} is allowed, then the one-neuron attack’s would have a potential to be successful in 100% of cases (see Fig. 4, right panel).

5 Conclusions and possible societal impact

In this work we reveal and analyse new adversarial vulnerabilities to which large-scale networks may be particularly susceptible. By design, research in this area looks at techniques that may be used to override the intended functionality of algorithms that are used within a decision-making pipeline, and hence may have serious negative implications in key sectors, including security, defence, finance and healthcare. By highlighting these shortcomings in the public domain, we raise awareness of the issue, so that both algorithm designers and end-users can be better informed. Our analysis of these vulnerabilities also identifies important factors contributing to their successful exploitation: *dimension* of the network’s latent space, *accuracy* of executing the attack (expressed by parameter α), and *over-parameterization*. These determinants enable us to propose model design strategies to minimise the chances of exploiting the adversarial vulnerabilities that we identified.

Low dimension of latent spaces. Our theoretical analysis suggests (bounds stated in Theorem 1 and Corollary 1) that the higher the dimension of latent spaces in state-of-the art deep neural networks the higher the chances of a successful attack. These chances approach one exponentially with dimension. One strategy to address this risk is to transform *wide* computational graphs in those parts of the network which are most vulnerable to open-box attacks into computationally equivalent *deeper but narrower* graphs. Such transformations can be done after the training and just before the model is shared or deployed. Another alternative is to employ dimensionality reduction approaches facilitating lower-dimensional layer widths during and after the training.

Constraining attack accuracy. An ability to find triggers with arbitrarily high accuracy is another component of the attacker’s success. Therefore increasing the computational costs of finding triggers for large enough δ with high accuracy is a viable defence strategy. A potential way could be to use gradient obfuscation techniques developed in the adversarial examples literature coupled with randomisation, as suggested in [19]. It is well-known that gradient obfuscation may not always prevent an attacker from finding a trigger [4]. Yet, making this process as complicated and computationally-intensive as possible would certainly contribute to increased security.

Reducing over-parameterization. We demonstrate theoretically and confirm in experiments that over-parameterization, inherent in many deep learning models, can easily be exploited by an adversary if models are freely shared and exchanged without control. In order to deny these opportunities to the attacker, removing susceptible neurons with our procedure in Section S.3.6 offers a potential remedy. More generally, employing network pruning [6, 7, 18, 25] as a part of model production pipelines would offer further protection against one-neuron attacks.

Network Hashing. In addition to the strategies above, which stem from theoretical analysis of stealth attacks, another defence could come from using fast network hashing algorithms executed in parallel with inference processes. The hash codes these algorithms produce will enable the owner to detect unwanted changes to the model after it was downloaded from a safe and trusted source.

Our theoretical and practical analysis of the new threats are in no way complete. In

experiments we assumed that pixels in images are real numbers. In reality though they may have to be integers. We did not assess how changes in numerical precision would affect the threat, and did not provide conditions when redundant neurons exist. Moreover, as we showed in Section S.3.5, our theoretical bounds could be conservative. Finally, vulnerabilities discovered here are intrinsically linked with AI maintenance problems discussed in [10]. Exploring these issues are topics for future research.

Nevertheless, the theory and empirical evidence which we present in this work make it clear that existing mitigation strategies must be strengthened in order to guard against vulnerability to new forms of stealth attack. Because the “inevitability” results that we derived have constructive proofs, our analysis offers promising options for the development of effective defences.

Acknowledgements

Desmond J. Higham was supported by grants EP/V046527/1 and EP/P020720/1 from the EPSRC; Alexander N. Gorban and Ivan Y. Tyukin were supported the Ministry of Science and Higher Education of the Russian Federation (Project No. 075-15-2020-808); Ivan Y. Tyukin was supported by the UKRI Turing AI Fellowship ARaISE EP/V025295/1 and UKRI Trustworthy Autonomous Systems Node in Verifiability EP/V026801/1.

References

- [1] Naveed Akhtar and Ajmal Mian. Threat of adversarial attacks on deep learning in computer vision: A survey. *IEEE Access*, 6:14410–14430, 2018.
- [2] Bibb Allen, Sheela Agarwal, Jayashree Kalpathy-Cramer, and Keith Dreyer. Democratizing AI. *Journal of the American College of Radiology*, 16:961–963, 2019.
- [3] Vegard Antun., Francesco Renna, Clarice Poon, Ben Adcock, and Anders C. Hansen. On instabilities of deep learning in image reconstruction and the potential costs of AI. *Proceedings of the National Academy of Sciences*, 117:30088–30095, 2020.
- [4] Anish Athalye, Nicholas Carlini, and David Wagner. Obfuscated gradients give a false sense of security: Circumventing defenses to adversarial examples. In *International Conference on Machine Learning*, pages 274–283. PMLR, 2018.
- [5] Battista Biggio and Fabio Roli. Wild patterns: Ten years after the rise of adversarial machine learning. *Pattern Recognition*, 84:317–331, 2018.
- [6] Davis Blalock, Jose Javier Gonzalez Ortiz, Jonathan Frankle, and John Gutttag. What is the state of neural network pruning? *arXiv preprint arXiv:2003.03033*, 2020.
- [7] Yu Cheng, Duo Wang, Pan Zhou, and Tao Zhang. A survey of model compression and acceleration for deep neural networks. *arXiv preprint arXiv:1710.09282*, 2017.
- [8] Javid Ebrahimi, Anyi Rao, Daniel Lowd, and Dejing Dou. HotFlip: White-box adversarial examples for text classification. In *Proceedings of the 56th Annual Meeting of the Association for Computational Linguistics (Volume 2: Short Papers)*, pages 31–36, Melbourne, Australia, July 2018. Association for Computational Linguistics.
- [9] S.G. Finlayson, J.D. Bowers, J. Ito, J. L. Zittrain, A. L. Beam, and I. S. Kohane. Adversarial attacks on medical machine learning. *Science*, 363:1287–1289, 2019.

- [10] A. N. Gorban, V. A. Makarov, and I. Y. Tyukin. The unreasonable effectiveness of small neural ensembles in high-dimensional brain. *Physics of Life Reviews*, pages 86–103, 2019.
- [11] AN Gorban and DA Rossiev. *Neural networks on personal computer*. Novosibirsk: Nauka (RAN), 1996.
- [12] Tianyu Gu, Brendan Dolan-Gavitt, and Siddharth Garg. Badnets: Identifying vulnerabilities in the machine learning model supply chain. *arXiv preprint arXiv:1708.06733*, 2017.
- [13] R.H.R. Hahnloser, R. Sarpeshkar, M.A. Mahowald, R.J. Douglas, and H.S. Seung. Digital selection and analogue amplification coexist in a cortex-inspired silicon circuit. *Nature*, 405(6789):947–951, 2000.
- [14] Catherine F. Higham and Desmond J. Higham. Deep learning: An introduction for applied mathematicians. *SIAM Review*, 61:860–891, 2019.
- [15] Xiaowei Huang, Daniel Kroening, Wenjie Ruan, James Sharp, Youcheng Sun, Min Thamo, Emeseand Wu, and Xinping Yi. A survey of safety and trustworthiness of deep neural networks: Verification, testing, adversarial attack and defence, and interpretability? *Computer Science Review*, 37, 2020.
- [16] Yann LeCun, Corinna Cortes, and Christopher J. C. Burges. The MNIST database of handwritten digits. Accessed June 17, 2019.
- [17] T. Liu, W. Wen, and Y. Jin. Sin2: Stealth infection on neural network — a low-cost agile neural trojan attack methodology. In *2018 IEEE International Symposium on Hardware Oriented Security and Trust (HOST)*, pages 227–230, 2018.
- [18] Evgeny M Mirkes. Artificial neural network pruning to extract knowledge. In *2020 International Joint Conference on Neural Networks (IJCNN)*, pages 1–8. IEEE, 2020.
- [19] Han Qiu, Yi Zeng, Qinkai Zheng, Tianwei Zhang, Meikang Qiu, and Gerard Memmi. Mitigating advanced adversarial attacks with more advanced gradient obfuscation techniques. *arXiv preprint arXiv:2005.13712*, 2020.
- [20] Kui Ren, Tianhang Zheng, Zhan Qin, and Xue Liu. Adversarial attacks and defenses in deep learning. *Engineering*, 6(3):346–360, 2020.
- [21] A. Shafahi, W.R. Huang, C. Studer, S. Feizi, and T. Goldstein. Are adversarial examples inevitable? *International Conference on Learning Representations (ICLR)*, 2019.
- [22] Ali Shafahi, Mahyar Najibi, Zheng Xu, John Dickerson, Larry S. Davis, and Tom Goldstein. Universal adversarial training. In *Proceedings of the AAAI Conference on Artificial Intelligence*, volume 34, pages 5636–5643, 2020.
- [23] Jiawei Su, Danilo Vasconcellos Vargas, and Kouichi Sakurai. One pixel attack for fooling deep neural networks. *IEEE Transactions on Evolutionary Computation*, 23:828–841, 2019.
- [24] Christian Szegedy, Wojciech Zaremba, Ilya Sutskever, Joan Bruna, Dumitru Erhan, Ian Goodfellow, and Rob Fergus. Intriguing properties of neural networks. *arXiv preprint arXiv:1312.6199*, 2013.

- [25] Hidenori Tanaka, Daniel Kunin, Daniel L Yamins, and Surya Ganguli. Pruning neural networks without any data by iteratively conserving synaptic flow. In H. Larochelle, M. Ranzato, R. Hadsell, M. F. Balcan, and H. Lin, editors, *Advances in Neural Information Processing Systems*, volume 33, pages 6377–6389. Curran Associates, Inc., 2020.
- [26] I.Y. Tyukin, D.J. Higham, and A.N. Gorban. On adversarial examples and stealth attacks in artificial intelligence systems. In *2020 International Joint Conference on Neural Networks (IJCNN)*, pages 1–6. IEEE, 2020.
- [27] I.Y. Tyukin, J.D. Higham, E. Woldegeorgis, and A.N. Gorban. Example code for open-box attacks. <https://github.com/tyukin/Stealth-adversarial-attacks>, 2021.
- [28] M. Wu, M. Wicker, W. Ruan and X. Huang, and M. Kwiatkowska. A game-based approximate verification of deep neural networks with provable guarantees. *Theoretical Computer Science*, 807:298–329, 2020.

Supplementary material

In this section we provide detailed proofs of our theoretical statements (Sections S.1, S.2), detailed description of procedures for finding triggers (Section S.3.1), discuss non-optimal choices of validation sets \mathcal{V} (Section S.3.2), and provide a detailed account of computational experiments (Sections S.3.3 – S.3.6).

All citations refer to References provided in the main body of the paper.

S.1 Proof of Theorem 1

The proof is split into 4 basic parts. We begin by *assuming* that latent representations $\mathbf{x}_i = \Phi(\mathbf{u}_i)$ of all elements \mathbf{u}_i from the set \mathcal{V} belong to the unit ball \mathbb{B}_n centered at the origin (for simplicity of notation unit n -ball centered at 0 is denoted as \mathbb{B}_n , and unit $n - 1$ sphere centered at 0 is denoted as \mathbb{S}_{n-1}). The main thrust of the proof is to establish lower bounds on the probability of the event

$$\mathcal{E}^*: \gamma(\mathbf{x}', \mathbf{x}') \geq (\mathbf{x}', \mathbf{x}_i) \text{ for all } \mathbf{x}_i = \Phi(\mathbf{u}_i) : \mathbf{u}_i \in \mathcal{V}, \mathbf{x}_i \in \mathbb{B}_n. \quad (\text{S.1})$$

These bounds are established in Parts 1 and 2. Then we proceed with constructing weights (both, input and output) and biases of the function g so that the modified map F_a delivers a solution of Problem 1. This is shown in *Part 3*. Finally, we remove the assumption that $\mathbf{x}_i \in \mathbb{B}_n$ and show how the weights and biases need to be adapted so that the adapted map F_a is a solution of Problem 1 for $\mathbf{x}_i \in \mathbb{B}_n(0, R)$ where $R > 0$ is a given number. This is demonstrated in *Part 4* of the proof.

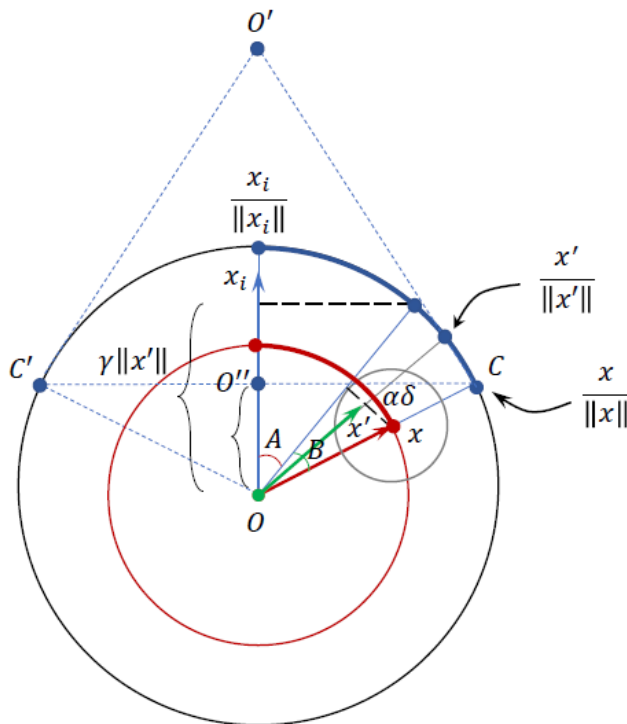


Figure S.1: To the proof of Theorem 1.

Part 1. Probability bound 1 on the event \mathcal{E}^ .* Let $\mathbf{x}_i, i = 1, \dots, M$ be an arbitrary element from \mathcal{V} , let \mathbf{x} be drawn randomly from an equidistribution in $\mathbb{S}_{n-1}(0, \delta)$, and let \mathbf{x}' be a vector that's within an $\alpha\delta$ -distance from \mathbf{x} :

$$\|x - x'\| \leq \alpha\delta.$$

Consider angles between $\mathbf{x}_i, \mathbf{x}'$ and \mathbf{x}', \mathbf{x} . Let

$$\begin{aligned} A^*(\mathbf{x}, \mathbf{x}_i) &= \min_{\mathbf{z}: \|\mathbf{x}-\mathbf{z}\| \leq \alpha\delta} |\angle(\mathbf{x}_i, \mathbf{z})|, \\ B^*(\mathbf{x}, \mathbf{x}_i) &= \max_{\mathbf{z}: \|\mathbf{x}-\mathbf{z}\| \leq \alpha\delta} |\angle(\mathbf{z}, \mathbf{x})| = |\angle(\mathbf{x}_i, \mathbf{x})| - A^*(\mathbf{x}, \mathbf{x}_i) \end{aligned}$$

(see Fig. S.1). It is clear that $A^*(\mathbf{x}, \mathbf{x}_i) \leq |\angle(\mathbf{x}_i, \mathbf{x}')|$ and $B^*(\mathbf{x}, \mathbf{x}_i) \geq |\angle(\mathbf{x}', \mathbf{x})|$. Notice that Algorithm 1 requests that $\gamma\|\mathbf{x}'\| \leq 1$ (i.e. $\arccos(\gamma\|\mathbf{x}'\|)$ always exists). Hence if the vector \mathbf{x} is chosen so that

$$A^*(\mathbf{x}, \mathbf{x}_i) \geq \arccos(\gamma\|\mathbf{x}'\|) \quad (\text{S.2})$$

then this choice would in turn guarantee that

$$\left(\frac{\mathbf{x}'}{\|\mathbf{x}'\|}, \frac{\mathbf{x}_i}{\|\mathbf{x}_i\|} \right) \leq \gamma\|\mathbf{x}'\|$$

(see Fig. S.1) and, consequently,

$$(\mathbf{x}', \mathbf{x}_i) \leq \gamma\|\mathbf{x}'\|^2\|\mathbf{x}_i\| = \gamma(\mathbf{x}', \mathbf{x}')\|\mathbf{x}_i\| \leq \gamma(\mathbf{x}', \mathbf{x}').$$

Observe that condition (S.2) is satisfied if

$$|\angle(\mathbf{x}_i, \mathbf{x})| \geq A + B = \arccos(\gamma\|\mathbf{x}'\|) + \arccos((1 - \alpha^2)^{1/2}),$$

where the values of angles A and B are $\arccos(\gamma\|\mathbf{x}'\|)$ and $\arccos((1 - \alpha^2)^{1/2})$, respectively (see Fig. S.1), and $A + B \in (0, \pi/2)$.

Let us denote

$$\beta(\gamma, \alpha, \|\mathbf{x}'\|) = \arccos(\gamma\|\mathbf{x}'\|) + \arccos((1 - \alpha^2)^{1/2}).$$

Given that parameters γ, δ, α are chosen so that (13) holds, it is clear that $0 < \beta(\gamma, \alpha, \|\mathbf{x}'\|) < \pi/2$.

One can therefore conclude that if the event

$$\mathcal{E} : \left(\frac{\mathbf{x}}{\|\mathbf{x}\|}, \frac{\mathbf{x}_i}{\|\mathbf{x}_i\|} \right) < \cos(\beta(\gamma, \alpha, \|\mathbf{x}'\|)) \text{ for all } \mathbf{x}_i \in \mathcal{V} \quad (\text{S.3})$$

occurs then the event \mathcal{E}^* , (S.1), must occur too.

Consider events

$$\mathcal{E}_i : \left(\frac{\mathbf{x}}{\|\mathbf{x}\|}, \frac{\mathbf{x}_i}{\|\mathbf{x}_i\|} \right) \geq \cos(\beta(\gamma, \alpha, \|\mathbf{x}'\|)).$$

The probability that \mathcal{E}_i occurs is equal to the area of the spherical cap

$$C(\mathbf{x}_i, \beta(\gamma, \alpha, \|\mathbf{x}'\|)) = \left\{ \mathbf{z} \in \mathbb{S}_{n-1} \mid \left(\frac{\mathbf{x}_i}{\|\mathbf{x}_i\|}, \mathbf{z} \right) \geq \cos(\beta(\gamma, \alpha, \|\mathbf{x}'\|)) \right\}$$

divided by the area of \mathbb{S}_{n-1} :

$$P(\mathcal{E}_i) = \frac{A_{n-1}(C(\mathbf{x}_i, \beta(\gamma, \alpha, \|\mathbf{x}'\|)))}{A_{n-1}(\mathbb{S}_{n-1})}. \quad (\text{S.4})$$

It is well-known that

$$A_{n-1}(C(\mathbf{x}_i, \beta(\gamma, \alpha, \|\mathbf{x}'\|))) = A_{n-2}(\mathbb{S}_{n-2}) \int_0^{\beta(\gamma, \alpha, \|\mathbf{x}'\|)} \sin^{n-2}(\theta) d\theta, \text{ and } A_{n-1}(\mathbb{S}_{n-1}) = \frac{2\pi^{\frac{n}{2}}}{\Gamma(\frac{n}{2})}.$$

Hence

$$P(\mathcal{E}_i) = \frac{A_{n-2}(\mathbb{S}_{n-2})}{A_{n-1}(\mathbb{S}_{n-1})} \int_0^{\beta(\gamma, \alpha, \|\mathbf{x}'\|)} \sin^{n-2}(\theta) d\theta.$$

Using the fact that inequality

$$P(\text{not } \mathcal{E}_1 \wedge \cdots \wedge \text{not } \mathcal{E}_M) \geq 1 - \sum_{i=1}^M P(\mathcal{E}_i) \quad (\text{S.5})$$

holds true for any events \mathcal{E}_i , that $\mathcal{E} = \text{not } \mathcal{E}_1 \wedge \cdots \wedge \text{not } \mathcal{E}_M$, and that $P(\mathcal{E}^*) \geq P(\mathcal{E})$ (as \mathcal{E} implies \mathcal{E}^*), we can conclude that

$$P((\mathbf{x}', \mathbf{x}_i) < \gamma(\mathbf{x}', \mathbf{x}') \text{ for all } \mathbf{x}_i \in \mathcal{V}) \geq 1 - M \frac{A_{n-2}(\mathbb{S}_{n-2})}{A_{n-1}(\mathbb{S}_{n-1})} \int_0^{\beta(\gamma, \alpha, \|\mathbf{x}'\|)} \sin^{n-2}(\theta) d\theta,$$

or, equivalently

$$P((\mathbf{x}', \mathbf{x}_i) < \gamma(\mathbf{x}', \mathbf{x}') \text{ for all } \mathbf{x}_i \in \mathcal{V}) \geq 1 - M \frac{1}{\pi^{\frac{1}{2}}} \frac{\Gamma(\frac{n}{2})}{\Gamma(\frac{n-1}{2})} \int_0^{\beta(\gamma, \alpha, \|\mathbf{x}'\|)} \sin^{n-2}(\theta) d\theta. \quad (\text{S.6})$$

Finally, noticing that

$$\beta(\gamma, \alpha, \|\mathbf{x}'\|) \leq \arccos(\gamma(1 - \alpha)\delta) + \arccos((1 - \alpha^2)^{1/2})$$

we can conclude that Algorithm 1 ensures that event \mathcal{E}^* , (S.1), occurs with probability at least (14).

Part 2. Probability bound 2 on the event \mathcal{E}^ .* Consider (S.4) and note that

$$P(\mathcal{E}_i) \leq \frac{A_{n-1}(C(\mathbf{x}_i, \arccos(\varphi(\gamma, \delta, \alpha))))}{A_{n-1}(\mathbb{S}_{n-1})}.$$

Recall that

$$A_{n-1}(C(\mathbf{x}_i, \arccos(\varphi(\gamma, \delta, \alpha)))) \frac{1}{n} = V_n(C(\mathbf{x}_i, \arccos(\varphi(\gamma, \delta, \alpha)))) + \frac{\varphi(\gamma, \delta, \alpha)}{n} V_{n-1} \left(B_{n-1} \left(\frac{\mathbf{x}_i}{\|\mathbf{x}_i\|} \varphi(\gamma, \delta, \alpha), (1 - \varphi(\gamma, \delta, \alpha)^2)^{1/2} \right) \right).$$

Observe that (see Fig. S.1) $|CO'|/|OO'| = |OO''|/|CO'|$. Given that $|CO'| = 1$ and $|OO'| = |OO''| + |O''O'|$,

$$|O''O'| + |OO''| = \frac{1}{|OO''|}, \text{ and } |O''O'| = \frac{1}{|OO''|} - |OO''|.$$

The above identity holds for all appropriate angles A and B , including for $A = \arccos(\gamma(1 - \alpha)\delta)$. That is, if $|OO''| = \varphi(\gamma, \delta, \alpha)$ then

$$|O''O'| = \frac{1}{\varphi(\gamma, \delta, \alpha)} - \varphi(\gamma, \delta, \alpha).$$

Notice that the spherical cap $C(\mathbf{x}', \varphi(\gamma, \delta, \alpha))$ is always inside the cone $C'CO$ whose base is the disc centered at $\frac{\mathbf{x}_i}{\|\mathbf{x}_i\|} \varphi(\gamma, \delta, \alpha)$ with radius $(1 - \varphi(\gamma, \delta, \alpha)^2)^{1/2}$. The height of this cone, according to the above calculations, is $\frac{1}{\varphi(\gamma, \delta, \alpha)} - \varphi(\gamma, \delta, \alpha)$. Therefore

$$V_n(C(\mathbf{x}', \varphi(\gamma, \delta, \alpha))) \leq \frac{1}{n} \left(\frac{1}{\varphi(\gamma, \delta, \alpha)} - \varphi(\gamma, \delta, \alpha) \right) \times V_{n-1} \left(B_{n-1} \left(\frac{\mathbf{x}_i}{\|\mathbf{x}_i\|} \varphi(\gamma, \delta, \alpha), (1 - \varphi(\gamma, \delta, \alpha)^2)^{1/2} \right) \right).$$

Hence

$$A_{n-1}(C(\mathbf{x}', \varphi(\gamma, \delta, \alpha))) \leq \frac{1}{\varphi(\gamma, \delta, \alpha)} V_{n-1}(\mathbb{B}_{n-1}) (1 - \varphi(\gamma, \delta, \alpha)^2)^{\frac{n-1}{2}}.$$

Taking into account that

$$\frac{V_{n-1}(\mathbb{B}_{n-1})}{A_{n-1}(\mathbb{S}_{n-1})} = \frac{\pi^{\frac{n-1}{2}}}{2\pi^{\frac{n}{2}}} \frac{\Gamma(\frac{n}{2})}{\Gamma(\frac{n-1}{2} + 1)} = \frac{1}{2\pi^{\frac{1}{2}}} \frac{\Gamma(\frac{n}{2})}{\Gamma(\frac{n}{2} + \frac{1}{2})},$$

we arrive at

$$P(\mathcal{E}_i) \leq \frac{1}{2\pi^{\frac{1}{2}}} \frac{\Gamma(\frac{n}{2})}{\Gamma(\frac{n}{2} + \frac{1}{2})} \frac{1}{\varphi(\gamma, \delta, \alpha)} (1 - \varphi(\gamma, \delta, \alpha)^2)^{\frac{n-1}{2}}. \quad (\text{S.7})$$

This confirms that event \mathcal{E}^* , (S.1), occurs with probability satisfying the bound (15).

Part 3. Construction of the structural adversarial perturbation. Having established bounds on the probability of event (S.1), let us now proceed with determining a map F_a which is solution to Problem 1 *assuming* that $\mathbf{x}_i \in \mathbb{B}_n$. Suppose that the event \mathcal{E}^* holds true:

$$(\mathbf{x}', \mathbf{x}_i) \leq \gamma \|\mathbf{x}'\|^2 \text{ for all } \mathbf{x}_i = \Phi(\mathbf{u}_i), \mathbf{u}_i \in \mathcal{V}, \mathbf{x}_i \in \mathbb{B}_n.$$

Set

$$\mathbf{w} = \kappa \mathbf{x}', \kappa > 0, \quad (\text{S.8})$$

$$b = \kappa \left(\frac{1+\gamma}{2} \right) \|\mathbf{x}'\|^2, \quad (\text{S.9})$$

and observe that

$$\mathfrak{A}(\cdot, (\mathbf{w}, b)) = Dg \left(\kappa \left((\cdot, \mathbf{x}') - \left(\frac{1+\gamma}{2} \right) \|\mathbf{x}'\|^2 \right) \right).$$

Recall that g is either ReLU or sigmoid and consider

$$\|F(\mathbf{x}_i) - F_a(\mathbf{x}_i, (\mathbf{w}, b))\| = |\mathfrak{A}(\cdot, (\mathbf{w}, b))|.$$

Since the function g is monotone,

$$|\mathfrak{A}(\mathbf{x}_i, (\mathbf{w}, b))| \leq Dg \left(-\kappa \left(\frac{1-\gamma}{2} \|\mathbf{x}'\|^2 \right) \right) \text{ for all } \mathbf{x}_i = \Phi(\mathbf{u}_i), \mathbf{u}_i \in \mathcal{V}, \mathbf{x}_i \in \mathbb{B}_n.$$

Denote

$$z = \frac{1-\gamma}{2} \|\mathbf{x}'\|^2$$

and pick the values of D and κ so that

$$Dg(-\kappa z) \leq \varepsilon \text{ and } Dg(\kappa z) \geq \Delta. \quad (\text{S.10})$$

Given that $\text{ReLU}(s) = 0$ for all $s \leq 0$ and that the sigmoidal function is strictly increasing with $g(0) \neq 0$, such choice is always possible.

Part 4. Generalisation to the case when $\mathbf{x}_i \in \mathbb{B}_n(0, R)$. Consider variables

$$\tilde{\mathbf{x}}_i = \frac{\mathbf{x}_i}{R}.$$

It is clear that $\tilde{\mathbf{x}}_i \in \mathbb{B}_n$. Suppose now that

$$(\mathbf{x}', \tilde{\mathbf{x}}_i) \leq \gamma \|\mathbf{x}'\|^2 \text{ for all } \tilde{\mathbf{x}}_i = \frac{\Phi(\mathbf{u}_i)}{R}, \mathbf{u}_i \in \mathcal{V}, \mathbf{x}_i = \Phi(\mathbf{u}_i) \in \mathbb{B}_n(0, R). \quad (\text{S.11})$$

Probability bounds on the above event have already been established in *Parts 1 and 2* of the proof.

Consider (S.8) from *Part 3* and re-scale the weight \mathbf{w} as follows:

$$\begin{aligned}\mathbf{w} &= \kappa \left(\frac{\mathbf{x}'}{R} \right), \quad \kappa > 0, \\ b &= \kappa \left(\frac{1+\gamma}{2} \right) \|\mathbf{x}'\|^2.\end{aligned}$$

This is equivalent to

$$\mathfrak{A}(\cdot, (\mathbf{w}, b)) = Dg \left(\kappa \left(\left(\frac{1}{R}, \mathbf{x}' \right) - \left(\frac{1+\gamma}{2} \right) \|\mathbf{x}'\|^2 \right) \right).$$

If the values of κ and D are chosen so that (S.10) in *Part 3* holds then

$$|\mathfrak{A}(\Phi(\mathbf{u}_i), (\mathbf{w}, b))| \leq \varepsilon \text{ for all } \mathbf{u}_i \in \mathcal{V}$$

and

$$\mathfrak{A}(\mathbf{x}'R, (\mathbf{w}, b)) = \mathfrak{A}(\Phi(\mathbf{u}'), (\mathbf{w}, b)) \geq \Delta.$$

This, together with bounds (S.6), (S.7) in *Parts 1 and 2* on the probability of event (S.11) concludes the proof. \square .

S.2 Proof of Corollary 1

Consider AI system (2) which satisfies Assumption 2. In addition to this system, consider a “virtual” one whose maps F and Φ are replaced with:

$$\tilde{\Phi}(\mathbf{u}) = \Phi(\mathbf{u}) - \Phi(\mathbf{u}^*), \quad \tilde{F}(\mathbf{x}) = F(\mathbf{x} + \Phi(\mathbf{u}^*)).$$

According to the definition of $\tilde{F} \circ \tilde{\Phi}$, domains of the definition of $\tilde{F} \circ \tilde{\Phi}$ and $F \circ \Phi$ coincide, and

$$\tilde{F} \circ \tilde{\Phi}(\mathbf{u}) = F \circ \Phi(\mathbf{u}) \text{ for all } \mathbf{u} \in \mathcal{U}. \quad (\text{S.12})$$

For this virtual system, $\tilde{F} \circ \tilde{\Phi}$, Assumption 1 is satisfied. Moreover, if an input \mathbf{u}'

$$\mathbf{x}' = \frac{\Phi(\mathbf{u}')}{R} - \frac{\Phi(\mathbf{u}^*)}{R}$$

satisfies conditions (9), (10) then these conditions are satisfied for $\mathbf{x}' = \tilde{\Phi}(\mathbf{u}')/R$ (the converse holds true too).

According to Theorem 1, adversarial perturbation defined by (11), (12):

$$\begin{aligned}\mathfrak{A} \left(\cdot, \left(\kappa \frac{\mathbf{x}'}{R}, b \right) \right) &= Dg \left(\left(\cdot, \kappa \frac{\mathbf{x}'}{R} \right) - b \right), \\ b &= \kappa \left(\frac{1+\gamma}{2} \right) \|\mathbf{x}'\|^2\end{aligned}$$

is a solution of Problem 1 for the virtual AI system $\tilde{F} \circ \tilde{\Phi}$, and probabilities of success are bounded from below as in (14), (15).

Notice that

$$\begin{aligned}\mathfrak{A} \left(\Phi(\mathbf{u}) - \Phi(\mathbf{u}^*), \left(\kappa \frac{\mathbf{x}'}{R}, b \right) \right) &= \\ Dg \left(\left(\Phi(\mathbf{u}), \kappa \frac{\mathbf{x}'}{R} \right) - \left(\kappa \left(\frac{1+\gamma}{2} \right) \|\mathbf{x}'\|^2 + \left(\Phi(\mathbf{u}^*), \kappa \frac{\mathbf{x}'}{R} \right) \right) \right).\end{aligned}$$

The latter expression, however, is identical to (11). Hence, taking (S.12) into account, we can conclude that Algorithm 2 returns a solution to Problem 1 for the original AI system $F \circ \Phi$ with probabilities of success satisfying (14), (15). \square

S.3 Additional material

S.3.1 Finding triggers \mathbf{u}' in Algorithms 1 and 2

A relevant optimisation problem for Algorithms 1 is formulated in (8). Similarly to (8), one can pose a constrained optimisation problem for finding a \mathbf{u}' in step 3 of Algorithm 2. This problem can be formulated as follows:

$$\begin{aligned} \mathbf{u}' = \arg \min_{\mathbf{u} \in \mathcal{U}} & \left\| \frac{\Phi(\mathbf{u})}{R} - \frac{\Phi(\mathbf{u}^*)}{R} - \mathbf{x} \right\| \\ \text{s. t.} & \\ \gamma \left\| \frac{\Phi(\mathbf{u})}{R} - \frac{\Phi(\mathbf{u}^*)}{R} \right\| & \leq 1, \quad \left\| \frac{\Phi(\mathbf{u})}{R} - \frac{\Phi(\mathbf{u}^*)}{R} - \mathbf{x} \right\| < \delta. \end{aligned} \quad (\text{S.13})$$

Note that the vector \mathbf{x} must be chosen randomly on $\mathcal{S}_{n-1}(0, \delta)$, $\delta \in (0, 1]$. One way to achieve this is to generate a sample \mathbf{z} from an n -dimensional normal distribution $\mathcal{N}(0, I_n)$ and then set $\mathbf{x} = \delta \mathbf{z} / \|\mathbf{z}\|$.

A possible practical approach to determine \mathbf{u}' now is to employ a gradient-based search

$$\mathbf{u}'_{k+1} = \text{Proj}_{\mathcal{U}} \left[\mathbf{u}'_k - \gamma_u(k) \frac{\partial}{\partial \mathbf{u}} \mathcal{L}(\mathbf{u}, \mathbf{u}^*) \right], \quad \mathbf{u}'_0 = \mathbf{u}^*,$$

where $\text{Proj}_{\mathcal{U}}$ is a projection operator. In our experiments, $\text{Proj}_{\mathcal{U}}(\mathbf{u})$ returned $\mathbf{u} = (u_1, \dots, u_n)$ if $u_i \in [0, 255]$. If, however, the i -th component of \mathbf{u} is out of range ($u_i < 0$ or $u_i > 255$) then the operator returned a vector with 0 or 255 in that corresponding component.

The loss function $\mathcal{L}(\mathbf{u}, \mathbf{u}^*)$ is defined as

$$\mathcal{L}(\mathbf{u}, \mathbf{u}^*) = \left\| \frac{\Phi(\mathbf{u})}{R} - \frac{\Phi(\mathbf{u}^*)}{R} - \mathbf{x} \right\|^2 + \lambda_1 \mathcal{G}_1(\mathbf{u}) + \lambda_2 \mathcal{G}_2(\mathbf{u}), \quad \lambda_1, \lambda_2 \geq 0,$$

and $\mathcal{G}_1, \mathcal{G}_2$ are relevant penalty functions:

$$\begin{aligned} \mathcal{G}_1(\mathbf{u}) &= \begin{cases} \left(\gamma \left\| \frac{\Phi(\mathbf{u})}{R} - \frac{\Phi(\mathbf{u}^*)}{R} \right\| - 1 \right)^{p_1}, & \gamma \left\| \frac{\Phi(\mathbf{u})}{R} - \frac{\Phi(\mathbf{u}^*)}{R} \right\| \geq 1 \\ 0, & \text{otherwise} \end{cases} \\ \mathcal{G}_2(\mathbf{u}) &= \begin{cases} \left(\left\| \frac{\Phi(\mathbf{u})}{R} - \frac{\Phi(\mathbf{u}^*)}{R} - \mathbf{x} \right\| - \delta \right)^{p_2}, & \left\| \frac{\Phi(\mathbf{u})}{R} - \frac{\Phi(\mathbf{u}^*)}{R} - \mathbf{x} \right\| \geq \delta \\ 0, & \text{otherwise} \end{cases} \end{aligned}$$

with parameters $p_1, p_2 > 0$, $\gamma_u(k) > 0$ is a parameter ensuring convergence of the procedure.

For Algorithm 1, terms $\Phi(\mathbf{u}^*)/R$ should be replaced with 0, and \mathbf{u}_0 can be set to an arbitrary element of \mathcal{U} .

Remark S.1 (Trigger search subspace) Finally, note that sometimes it may be feasible to sample \mathbf{x} in step 2 of Algorithm 2 from a $S_{m-1}(0, \delta) \subset \mathbb{R}^n$, $2 \leq m < n$ instead of $S_{n-1}(0, \delta)$. On the one hand this will have a negative affect on the probability of success as n would need to be replaced with $2 \leq m < n$ in (14) and (15). On the other hand this extra “pre-processing” step may enable us to lower the values of α .

Indeed, if $\Phi(\mathbf{u}^*)$ is an output of a ReLU layer then it is likely that some of it’s components are exactly zero. This would constrain gradient-based approaches to determine \mathbf{u}' starting from \mathbf{u}^* if \mathbf{x} is sampled from $S_{n-1}(0, \delta)$ as the corresponding gradients will always be equal to zero. In our code [27] illustrating the application of Algorithms 1, 2 we implement this pre-processing strategy.

S.3.2 Success bounds and a “concentrational collapse” for a class of validation sets \mathcal{V}

Consider an AI system with an input-output map (2). Let an input \mathbf{u}^* (available to the attacker) and a validation set \mathcal{V} , $|\mathcal{V}| = M$ (unknown to the attacker), be such that

$$\|\Phi(\mathbf{u}^*) - \Phi(\mathbf{u}_i)\| \leq R \text{ for all } \mathbf{u}_i \in \mathcal{V}.$$

In addition, suppose that both the validation set and the input \mathbf{u}^* satisfy Assumption S.1 below

Assumption S.1 (Data model) *Elements $\mathbf{u}_1, \dots, \mathbf{u}_M$ and \mathbf{u}^* are drawn from a family of distributions P_1, \dots, P_M and P^* satisfying the following properties:*

1. *There is a $\mathbf{c} \in \mathbb{R}^n$ such that $\mathbf{u}_1, \dots, \mathbf{u}_M$ are always in the set:*

$$\{\mathbf{u} \in \mathcal{U} \mid \|\Phi(\mathbf{u}) - \mathbf{c}\| \leq R/2\}. \quad (\text{S.14})$$

2. *There is a $C \geq 0$ such that*

$$\begin{aligned} P_i(\Phi(\mathbf{u}_i) \in \mathbb{B}_n(\Phi(\mathbf{u}), r) \mid \mathbf{u}_1, \dots, \mathbf{u}_M) &\leq C \left(\frac{2r}{R} \right)^n, \\ P^*(\Phi(\mathbf{u}^*) \in \mathbb{B}_n(\mathbf{c}, r) \mid \mathbf{u}_1, \dots, \mathbf{u}_M) &\leq C \left(\frac{2r}{R} \right)^n, \end{aligned} \quad (\text{S.15})$$

for all $\mathbf{u} \in \mathcal{U}$.

Property (S.14) requests that the validation set is mapped into a ball centered at $\Phi(\mathbf{c})$ and having a radius $R/2$ in the system’s latent space, and (S.15) is a non-degeneracy condition restricting pathological concentrations.

As we show below, if the validation set satisfies Assumption S.1 and the attacker uses Algorithm 2 with \mathbf{u}^* drawn from a distribution P^* satisfying conditions of Assumption S.1, then the probabilities of generating a successful attack may be drastically increased.

Theorem S.1 *Consider Algorithm 2, and let parameters $\gamma \in (0, 1)$, $\alpha \in [0, 1)$, and $\delta \in (0, 1]$ be such that (13) holds. Furthermore, suppose that $\gamma\delta < 1/2$ and let Assumption S.1 hold.*

Then the probability $P_{a,1}$ that Algorithm 2 returns a solution to Problem 1 is bounded from below as:

$$\begin{aligned} P_{a,1} &\geq P_a(\epsilon), \quad \epsilon \in [0, \gamma\delta] \\ P_a(\epsilon) &= 1 - C(1 - 2\epsilon)^n - M \frac{C}{2} \left[2 \left(\frac{1}{4} - \left(\frac{1}{2} - \epsilon - \gamma\delta \right)^2 \right)^{1/2} \right]^n \\ &\quad - \pi^{-1/2} \frac{\Gamma\left(\frac{n}{2}\right)}{\Gamma\left(\frac{n-1}{2}\right)} \int_0^{\arccos(\varphi(\gamma, \delta, \alpha))} \sin^{n-2}(\theta) d\theta. \end{aligned} \quad (\text{S.16})$$

Proof of Theorem S.1. The proof is essentially presented in Fig S.2.

Consider the following three events

$$\text{Event 1 : } \mathbf{u}^* : \|\Phi(\mathbf{u}^*) - \mathbf{c}\| \leq R/2 - \epsilon R,$$

Event 2 : for an element $\mathbf{u}_i \in \mathcal{V}$,

$$\Phi(\mathbf{u}_i) \in C^* = \left\{ \mathbf{x} \in \mathbb{B}_n(\mathbf{c}, R/2) \mid \left(\frac{\Phi(\mathbf{u}^*) - \mathbf{c}}{\|\Phi(\mathbf{u}^*) - \mathbf{c}\|}, \mathbf{x} - \mathbf{c} \right) \geq R \left(\frac{1}{2} - (\epsilon + \gamma\delta) \right) \right\}$$

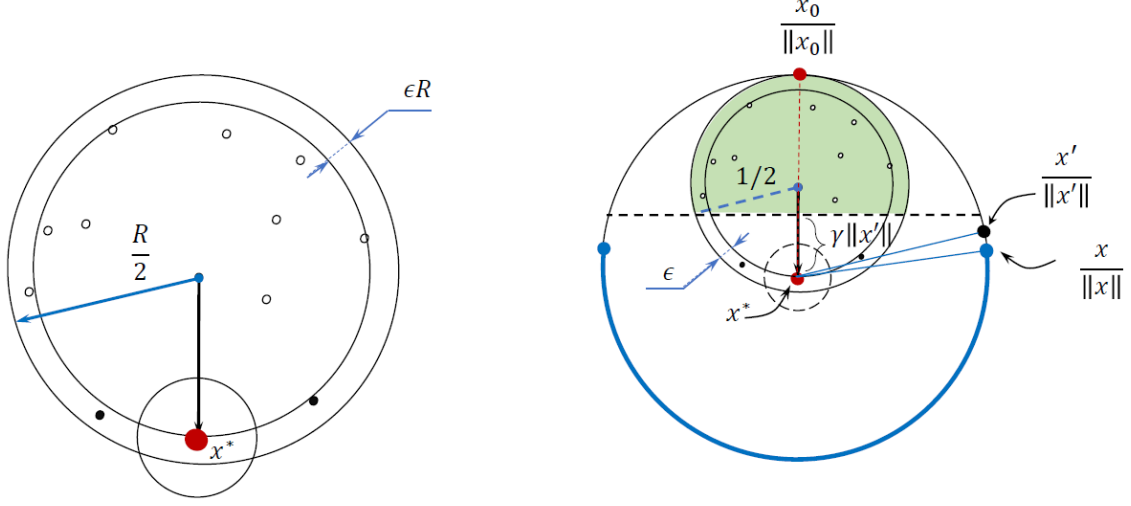


Figure S.2: Concentrational collapse of unknown verification sets. Shaded green area shows elements $\mathbf{u} \in \mathcal{V}$ for which $((\Phi(\mathbf{u}) - \Phi(\mathbf{u}^*)) / R, \mathbf{x}' / \|\mathbf{x}'\|) \geq \gamma \|\mathbf{x}\|$. Vectors $\mathbf{x}^* = \Phi(\mathbf{u}^*)$ show latent representations of \mathbf{u}^* , small circles show $\Phi(\mathbf{u}_i)$ (both, black and white). Filled black circles show elements of \mathcal{V} which do not satisfy this condition.

and

$$\text{Event 3 : } \cos(|\angle(\mathbf{x}', \mathbf{x}_0)|) \geq \gamma \delta (1 - \alpha).$$

The probability that Event 1 holds is bounded as

$$P(\text{Event 1}) = P(\mathbf{u}^* \in \mathbb{B}_n(\mathbf{c}, R/2 - \epsilon R)) \leq C(1 - 2\epsilon)^n.$$

The probability of Event 2 is does not exceed the probability that $\Phi(\mathbf{u}_i)$ belongs to a half-ball of radius

$$R \left(\frac{1}{4} - \left(\frac{1}{2} - \epsilon - \delta \gamma \right)^2 \right)^{1/2}$$

and hence

$$P(\text{Event 2}) \leq \frac{C}{2} \left[2 \left(\frac{1}{4} - \left(\frac{1}{2} - \epsilon - \delta \gamma \right)^2 \right)^{1/2} \right]^n.$$

The probability that Event 3 holds is bounded from above by

$$P(\text{Event 3}) \leq \pi^{-1/2} \frac{\Gamma\left(\frac{n}{2}\right)}{\Gamma\left(\frac{n-1}{2}\right)} \int_0^{\arccos(\varphi(\gamma, \delta, \alpha))} \sin^{n-2}(\theta) d\theta$$

(see proof of Theorem 1 for details). If none of these events hold then Algorithm 2 produces a solution to Problem 1. The probability when this occurs is bounded from below as (S.16) (see (S.5)). \square

Theorem S.1 reveals a phenomenon where validation sets which could be deemed as sufficiently large in the sense of bounds specified by Theorem 1 and Corollary 1 may still be considered as “small” due to bound (S.16). We call this phenomenon *concentrational collapse*. When concentrational collapse occurs, the AI system becomes particularly vulnerable to small validation sets \mathcal{V} even when the attacker’s accuracy is small (α large). For example for $n = 200$, $\epsilon = 0.01$, $\gamma = 0.9$, $\delta = 1/3$

$$P(\text{Event 2}) \leq C 8.4343 \times 10^{-8}$$

Table S.1: Network architecture used in experiments. Red color shows layers which we represent by map \mathcal{F} in (1)

Layer number	Type	Size
1	Input	$28 \times 28 \times 1$
2	Conv2d	$3 \times 3 \times 8$
3	Batch normalization	
4	ReLU	
5	Maxpool	pool size 2×2 , stride 2×2
6	Conv2d	$3 \times 3 \times 16$
7	Batch normalization	
8	ReLU	
9	Maxpool	pool size 2×2 , stride 2×2
10	Conv2d	$3 \times 3 \times 32$
11	Batch normalization	
12	ReLU	
13	Fully connected	200
14	ReLU	
15	Fully connected	100
16	ReLU	
17	Fully connected	10
18	Softmax	10

implying that the owner would have to generate and keep a rather large validation set \mathcal{V} to make up for these small probabilities.

In view of Remark S.1, when the vector \mathbf{x} is drawn from $\mathbb{S}_{n_p-1}(0, \delta)$, $2 \leq n_p < n$, bound (S.16) becomes:

$$\begin{aligned}
P_{a,1} &\geq P_a(\epsilon), \quad \epsilon \in [0, \gamma\delta] \\
P_a(\epsilon) &= 1 - C(1 - 2\epsilon)^n - M \frac{C}{2} \left[2 \left(\frac{1}{4} - \left(\frac{1}{2} - \epsilon - \gamma\delta \right)^2 \right)^{1/2} \right]^n \\
&\quad - \pi^{-1/2} \frac{\Gamma\left(\frac{n_p}{2}\right)}{\Gamma\left(\frac{n_p-1}{2}\right)} \int_0^{\arccos(\varphi(\gamma, \delta, \alpha))} \sin^{n_p-2}(\theta) d\theta.
\end{aligned} \tag{S.17}$$

S.3.3 Architecture and training parameters of deep convolutional neural networks used in experiments

Architecture of a deep convolutional neural network which we used in our experiments is shown in Table S.1. The architecture features 3 fully connected layers, with layers 15 – 18 (shown in red) and layers 1 – 14 representing maps F and Φ , respectively.

This architecture is built on a standard benchmark example from Mathworks. The original basic network was appended by layers 13 – 16 to emulate dense fully connected structures present in popular deep learning models such as VGG16, VGG19. Note that the last 6 layers (layers 13 – 18) are in fact 3 dense layers with ReLU, ReLU, and softmax activation functions, respectively, if the same network is implemented in Tensorflow-Keras. Having 3 dense layers is not essential for the method, and the attacks can be implemented in other networks featuring ReLU or sigmoid neurons.

Outputs of the softmax layer assign class label to images. Label 1 corresponds to digit “0”, label 2 to digit “1”, and label 10 to digit “9”, respectively.

Training. The original MNIST dataset of 10,000 images was split into a training set consisting of 7,500 images and a test set containing 2,500 images (see example code for details of implementation [27]). The network was trained over 30 epochs with the minibatch size parameter set to 128 images, and with a momentum version of the stochastic gradient descent. The momentum parameter was set to 0.9 and the learning rate was $0.01/(1+0.001k)$, where k is the training instance’s number within an epoch.

Overall, we conducted 20 attack experiments involving determining different trigger-target pairs and changing the network’s architecture in accordance with planting scenarios 1 and 3. The original networks’ classification accuracy (before the attack), expressed as the percentage of correct classifications on the test set, was within [98.64%, 99.84%] in all these 20 experiments.

Computational environment and indicative compute resources. All experiments were performed in MATLAB2020b on an HP Zbook 15 G3 laptop with a Core i7-6820HQ CPU, 16 Gb of RAM and Nvidia Quadro 1000M GPU. Training a single instance of a network in this environment took approximately 300 seconds. Running a section of the code in [27] implementing 100,000 gradient steps to determine a trigger input took about 3400 seconds, and a part of the code determining which neuron to attack took about 95 seconds. These figures varied marginally from one run to another.

S.3.4 Trigger and target images

In addition to examples of triggers shown in Fig. 3, we generated triggers to all digits 0 – 9. These triggers, \mathbf{u}' , as well as the original images (target images), \mathbf{u}^* , are shown in S.3. As is evident from these figures, triggers retain significant resemblance of the original target images \mathbf{u}^* .

Moreover, when trigger images were shown to the original networks (i.e. trained networks *before* we subjected them to stealth attacks produced by Algorithm 2), in many cases these network returned class labels which coincided with class labels of the target images. A summary of this test is provided in Figure S.4. Red colour highlights instances when the networks’ original classifications of the target images did not match those of the trigger. In these 20 experiments target images of digits from 0 to 9 were chosen at random. In each row, the number of entries in the second column in the table in Figure S.4 corresponds to the number of times the digit in the first column was chosen as a “target” in these experiments.

S.3.5 Accuracy of implementation of stealth attacks achieved in experiments and limits of theoretical bounds in Theorem 1 and Corollary 1

In all 20 attack experiments we were able to create a ReLU neuron which was completely silent on the set \mathcal{V} and, at the same time, was producing desired responses when a trigger was presented as an input to the network. Empirical values of the accuracy of implementation of these attacks, α and dimension n of the random perturbation are shown in Table S.2.

These figures, along with the fact that all these attacks returned a successful outcome (for Scenario 1), enable us to illustrate how conservative the bounds provided in Theorem 1 could be.

Indeed, computing the term

$$P_1(\alpha, \delta, \gamma, n) = \pi^{-1/2} \frac{\Gamma\left(\frac{n}{2}\right)}{\Gamma\left(\frac{n-1}{2}\right)} \int_0^{\arccos(\varphi(\gamma, \delta, \alpha))} \sin^{n-2}(\theta) d\theta$$

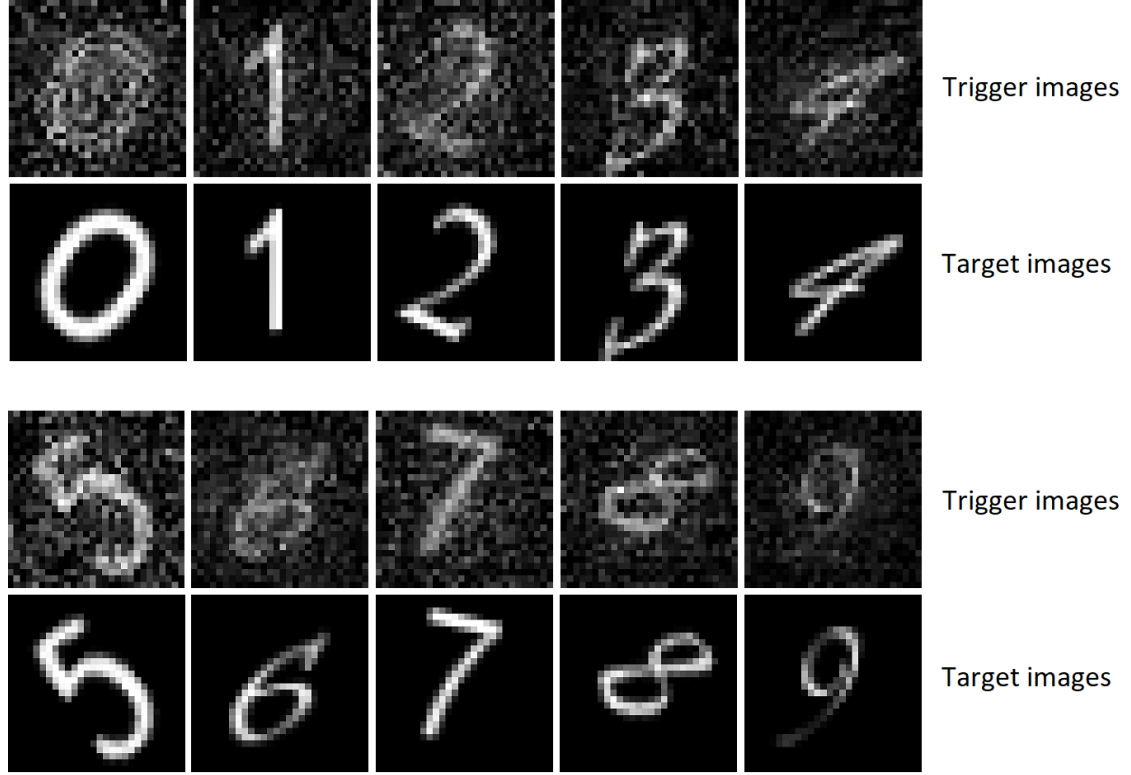


Figure S.3: Examples of trigger images \mathbf{u}' (rows 1 and 3) and their corresponding "target images" \mathbf{u}^* (rows 2 and 4).

Target image of the trigger	Predicted label
0	0, 3
1	4 , 7
2	2
3	3
4	4,4
5	5
6	6,6,6
7	7
8	8, 5 , 6 , 9
9	9,9,9

Figure S.4: Retained information content in the trigger images

#	1	2	3	4	5	6	7	8	9	10
α	0.179	0.200	0.358	0.247	0.313	0.406	0.311	0.277	0.362	0.244
n	112	125	122	116	125	122	115	121	128	111

#	11	12	13	14	15	16	17	18	19	20
α	0.417	0.271	0.271	0.227	0.246	0.287	0.401	0.327	0.436	0.285
n	122	124	124	119	110	117	120	109	110	117

Table S.2: Accuracy α of finding triggers expressed as $\alpha = \delta^{-1} \|\Phi(\mathbf{u}')/R - \mathbf{x}\|$.

for $\gamma = 0.9$ in bound (14) for α, n taken from the first experiment in Table S.2 (column corresponding to $\# = 1$) returns $P_1(\alpha, \delta, \gamma, n) = 0.1561$. Substituting this figure into (14) for $M > 10$ produces a negative number rendering the bound not useful in this case. The same comment applies to other experiments. At the same time, as our experiments confirm, the attacks turn out to be successful in practice. If, however, we set $\alpha = 0$ then the value of $P_1(0, \delta, \gamma, n)$ for the first experiment becomes 4.9180×10^{-4} .

These observations highlight limitations of bounds in Theorem 1 and Corollary 1 for determining probabilities of success in practice when the values α are large. They also show additional relevance of Theorem S.1 and the “concentrational collapse” effect for developing better understanding of stealth attacks. Indeed, applying bound (S.17) with $n = 200$, $\epsilon = 0.02$, $\gamma = 0.9$ and $n_p = 112$, $\alpha = 0.179$ (first row from Table S.2) one obtains:

$$P_{a,1} \geq 1 - C \times 2.8461 \times 10^{-4} - MC \times 4.6866 \times 10^{-7} - 0.1561.$$

If parameter C does not exceed 100 then this latter bound is more consistent with what we observed in experiments. Its validity, however, too depends on Assumption S.1 about the distributions from which the set \mathcal{V} and \mathbf{u}^* are sampled from.

S.3.6 Selection of a neuron to attack

Let L be the layer in which a neuron is to be selected for the attack. We suppose that the network has a layer $L + 1$ in its computational graph. Suppose that $w_{i,j}^{[L]}$ denotes the j -th weight of the i -th neuron in layer L , and the total number of neurons in layer L is N_L .

We say that the *output* weight vector of the i -th neuron in layer L is a vector

$$\bar{\mathbf{w}}_i^{[L]} = \begin{pmatrix} w_{1,i}^{[L+1]} \\ w_{2,i}^{[L+1]} \\ \vdots \\ w_{N_L,i}^{[L+1]} \end{pmatrix}.$$

Determining neurons’ ranks. For each $i = 1, \dots, N_L$, we computed L_1 -norms of $\bar{\mathbf{w}}_i^{[L]}$:

$$\|\bar{\mathbf{w}}_i^{[L]}\|_1 = \sum_{j=1}^{N_{L+1}} |w_{j,i}^{L+1}|$$

and created a list of indices n_1, n_2, \dots, n_{N_L} such that

$$\|\bar{\mathbf{w}}_{n_1}^{[L]}\|_1 \leq \|\bar{\mathbf{w}}_{n_2}^{[L]}\|_1 \leq \dots \leq \|\bar{\mathbf{w}}_{n_{N_L}}^{[L]}\|_1.$$

Susceptibility rank of the i -th neuron, $\text{Rank}(i)$, is defined as a number $k \in \{1, \dots, N_L\}$:

$$\text{Rank}(i) = k : i = n_k.$$

If the above holds for multiple values of $n_k : n_{k_1}, n_{k_2}, \dots, n_{k_m}$ then the neuron’s rank is determined by selecting a single number from k_1, \dots, k_m at random.

In our experiments, when implementing stealth attacks in accordance with Scenario 3, we always selected neurons whose susceptibility rank is 1.